NONLINEAR EFFECTS IN SOI MICRO-RING RESONATORS

Andreea FAZACAŞ[1], Paul STERIAN[2]

By using the Finite Difference Time-Domain Method (FDTD), nonlinear effects in ring resonator were studied. FDTD Method is a powerful mathematical tool to solve Maxwell equations in micro-structured optical devices, in our case. These devices have various applications ranging from filters to ultrafast signal processing and sensing.

In this paper we studied two types of dispersive effects in nonlinear materials of a SOI (Silicon on insulator) micro-ring resonator: second-order effect and third order effect. SOI micro-rings are of particular interest due to their operation wavelength near 1.55 μm, due to their optical confinement and due to their low cost for microelectronics integration.

In our simulations we used different wavelengths, in order to obtain high quality factors of the micro-ring resonators, but also to determine the applications of these photonic structures.

This method can be used by designers to obtain optimal parameters for their applications.

Keywords: micro-ring resonators, nonlinear effects, SOI, FDTD

1. Introduction

Solving Maxwell equations by Finite-Difference Time-Domain (FDTD) Method was of great interest in late years, due to the simple implementation in software simulations. This mathematical method was used in a variety of photonic based studies [1-6]. Previous work of authors analyzed the second and third order dispersion effects in optical fibers [7, 21] by using another numerical method (Split-Step Fourier Method).

By using FDTD Method, Hagness et all. described, in their work [4,13-18], the design and experimental realization of a simple ring-resonator. Modelling micro-ring resonators is of great importance, due to this type of devices to offer a large free spectral range, but also a narrow band.

If the power density of the light is large, then the nonlinear effects will appear in materials. Nonlinear analysis has been used intensively in the last years,

[1]PhD Student, Academic Center of Optical Engineering and Photonics, University POLITEHNICA of Bucharest, 313 Spl. Independentei, 060042 Bucharest, Romania; e-mail: a.fazacas@ifa-mg.ro
[2]Prof., Physics Department, University POLITEHNICA of Bucharest, 313 Spl. Independentei, 060042 Bucharest, Romania; e-mail: sterian@physics.pub.ro

due to its importance in a variety of applications, even at low power levels. Also, the study of nonlinearities in ring-resonators is of great importance since the intensity in the waveguide is much lower than the intensity in the ring.

The linear and nonlinear characteristics of optical slow-wave structures made of direct coupled Fabry-Pérot and ring-resonators were discussed by Mellonini et all. [6] in 2003. Also, in this paper there are suggested a series of applications, where the slow-wave propagation can increase the performance of the modern optical devices [6,19]. Another study presents the modelling of the dispersive nonlinear effects in ring-resonators [7,14].

Nonlinear effects can occur, also, in silica even at modest input powers. These effects occur due to the confinement of the light in the narrow core of the waveguides. A particular study revealed that silicon micro-rings can be used for optical manipulation [9].

The Silicon on Insulator (SOI) technology was used lately to reduce the parasitic device capacitance. The effect of the reduced capacitance is the performance improvement of the photonic device. Also, this material can be easily integrated in photonic devices, due to their compact dimensions. A large bandwidth for slow light devices in cascade passive silicon on insulator micro-rings was obtained by Yuntao et all. The obtained results were remarkable: a 57 ps group delay and an 83 Gbps bit rate was suggested according the measured 3dB spectral bandwidth in the 8-stage cascaded micro-rings [7].

The nonlinear behaviour in a 200 mm SOI wafer with a thickness of the Silicon layer of 220 nm and buried oxide of 1 μm was studied by Priem et all. They demonstrate optical bistability for input powers as low as 0,277 mW [8]. Another study reveals the cascade excitability in a micro-ring with high quality factor, which at certain wavelengths (blue light) undergoes a subcritical Andronov-Hopf bifurcation. If the input light is red, in the bistability region, a supercritical Andronov-Hopf bifurcation occur [9-12].

In this study we simulated the amplitude for a simple ring-resonator coupled to a single waveguide. First, we used a SOI based micro-ring resonator. Then we changed the material of the waveguide to be nonlinear. This paper studies the second order and third order nonlinearities in SOI based micro-ring resonators. Nonlinear effects induced major changes in the quality factors of the micro-ring resonators. Our simulations were made with OptiFDTD Software [13, 22-23] for different resonant wavelengths.

2. Mathematical background

The simplest configuration of a micro-ring resonator consists of a unidirectional coupling between a waveguide and a ring resonator, as we can see in Fig. 1 [13].

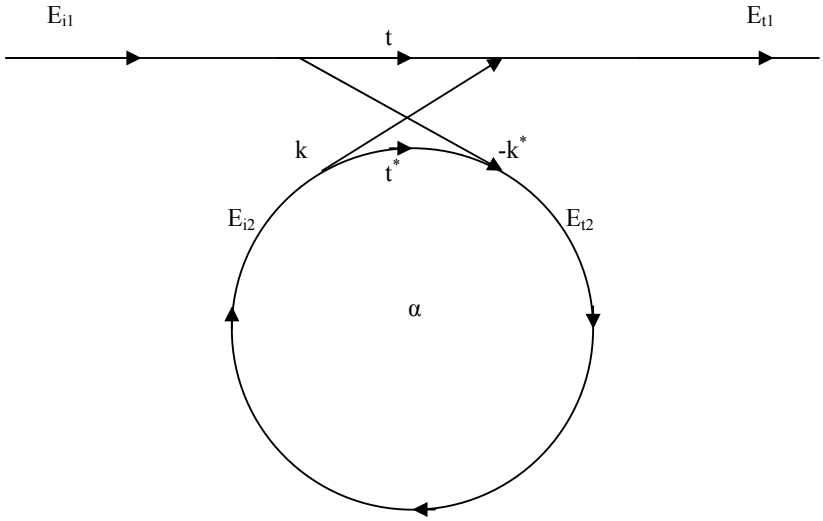

Fig. 1. Single micro-ring resonator with single waveguide.

The simplest micro-ring resonator is described by the following matrix relation:

$$\begin{pmatrix} E_{t1} \\ E_{t2} \end{pmatrix} = \begin{pmatrix} t & k \\ -k^* & t^* \end{pmatrix} \begin{pmatrix} E_{i1} \\ E_{i2} \end{pmatrix}, \tag{1}$$

where E_{t1} and E_{t2} are the transmitted fields in the ring and in the waveguide, E_{i1} and E_{i2} are the input fields in the waveguide and in the ring, t and k are the coupler parameters and the * represents the complex value of t and k [10].

If we chose $E_{i1} = 1$ then the round trip in the ring resonator will be given by the following relation:

$$E_{i2} = \alpha \cdot e^{j\theta} E_{t2}, \tag{2}$$

where α is the loss coefficient of the ring, $\theta = \omega L/c$, L being the circumference of the ring and c the phase velocity of the ring mode and the fixed angular frequency $\omega = k_1 c_0$, c_0 the speed of light in vacuum and $k_1 = 2\pi/\lambda$ is the vacuum wave number.

The ring coupling relations are given by:

$$\beta = \frac{2\pi n_{eff}}{\lambda}, \qquad \theta = \frac{4\pi n_{eff} r}{\lambda} \tag{3}$$

where β is the propagation constant, n_{eff} is the effective refractive index, λ is the wavelength of the laser, θ is the phase shift per circulation and r is the ring radius measured from the center of the ring to the center of the waveguide [13].

From this we obtain the other components of the field:

$$E_{t1} = \frac{-\alpha + t \cdot e^{-j\theta}}{-\alpha t^{*} + \cdot e^{-j\theta}}$$
$$E_{t2} = \frac{-k^{*}}{1 - \alpha t^{*} \cdot e^{j\theta}} \tag{4}$$
$$E_{i2} = \frac{-\alpha k^{*}}{-\alpha t^{*} + \cdot e^{-j\theta}}$$

The transmission power in the output waveguide and the circulating power in the ring will be:

$$P_{t1} = \left|E_{t1}\right|^2 = \frac{\alpha^2 + \left|t\right|^2 - 2\alpha\left|t\right|\cos(\theta + \varphi_t)}{1 + \alpha^2\left|t\right|^2 - 2\alpha\left|t\right|\cos(\theta + \varphi_t)}$$
$$P_{i2} = \left|E_{i2}\right|^2 = \frac{\alpha^2(1 - \left|t\right|^2)}{1 + \alpha^2\left|t\right|^2 - 2\alpha\left|t\right|\cos(\theta + \varphi_t)} \tag{5}$$

where $|t|$ is the coupling losses and φ_t the phase of the coupler [13].

On the resonance equation (5) becomes:

$$P_{t1} = \left|E_{t1}\right|^2 = \frac{(\alpha - \left|t\right|)^2}{(1 - \alpha\left|t\right|)^2}$$
$$P_{i2} = \left|E_{i2}\right|^2 = \frac{\alpha^2(1 - \left|t\right|^2)}{(1 - \alpha\left|t\right|)^2} \tag{6}$$

If we have zero losses in the ring (α = 1) we can see that all the power remains in the ring and that nothing passes into the waveguide (P_{tl} is equal to zero for all $|t|^2$). The ring-resonator may be used as band stop filter (Fig. 2.).

If the losses in the ring are at the maximum (α = *0*) all the signal passes through the waveguide, but nothing passes into the ring. In this case, P_{tl} increases strongly with the increase of the coupling losses coefficient. The waveguide may be used for telecommunication applications (Fig. 2.).

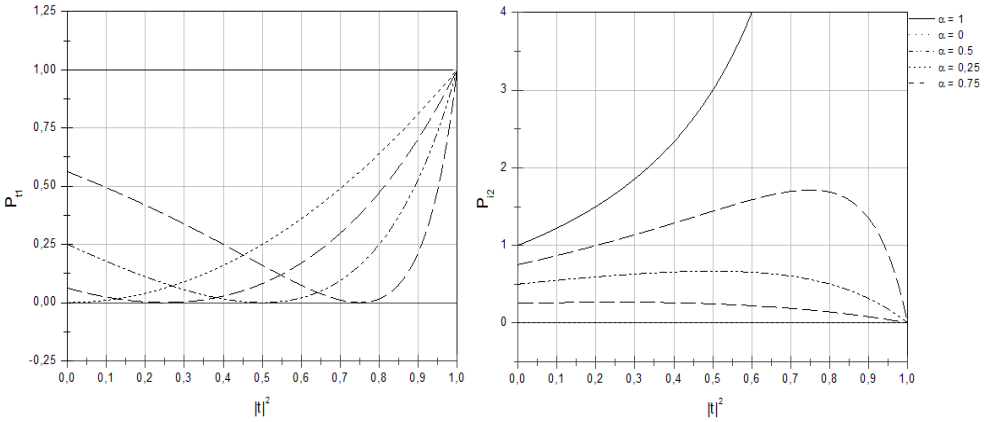

Fig. 2. The transmission power at the output of the waveguide (P_{t1}) and the circulating power in the ring (P_{i2}), for different values of the loss coefficient in the ring α.

To describe the FDTD algorithm we consider a region of space with no electric or magnetic current sources. Consequently, the time-dependent Maxwell's equations are described by the following equations:

$$\frac{\partial \vec{B}}{\partial t} = -\nabla \times \vec{E} - \vec{M}\ ; \frac{\partial \vec{D}}{\partial t} = \nabla \times \vec{H} - \vec{J}\ ; \nabla \cdot \vec{D} = 0\ ;\ \nabla \cdot \vec{B} = 0\ , \tag{7}$$

where $\vec{E}$ is the electric field (V/m), $\vec{D}$ is the electric flux density (C/m^2), $\vec{H}$ is the magnetic field (A/m), $\vec{B}$ is the magnetic flux density (Wb/m^2), and $\vec{J}$ is the electric current density (A/m^2) [1-2].

We can relate $\vec{D}$ to $\vec{E}$ and $\vec{B}$ to $\vec{H}$ using the relations:

$$\vec{D} = \varepsilon \vec{E} = \varepsilon_r \varepsilon_0 \vec{E}\ ;\ \vec{B} = \mu \vec{H} = \mu_r \mu_0 \vec{H}\ , \tag{8}$$

where ε (F/m), ε_r is the relative permittivity, ε_0 is the free-space permittivity (8.85×10^{-12}), μ is the magnetic permeability (H/m), μ_r is the relative permeability, and μ_0 is the free-space permeability ($4\pi \times 10^{-7}$ H/m) [1-3].

$\vec{J}$ and $\vec{M}$ can act as independent sources of $\vec{E}$ and $\vec{H}$ field energy and can be written as:

$$\vec{J} = \vec{J}_{source} + \sigma \vec{E};\qquad \vec{M} = \vec{M}_{source} + \sigma^* \vec{H} \tag{9}$$

where σ is the electric conductivity (S/m) and σ^* is the magnetic loss (Ω / m). Using (7), (8) and (9) we obtain the Maxwell's curl equations in linear, isotropic, non-dispersive, lossy materials:

$$\begin{aligned} \frac{\partial \vec{H}}{\partial t} &= -\frac{1}{\mu} \nabla \times \vec{E} - \frac{1}{\mu} \left(\vec{M}_{source} + \sigma^* \vec{H} \right) \\ P \frac{\partial \vec{E}}{\partial t} &= \frac{1}{\varepsilon} \nabla \times \vec{H} - \frac{1}{\varepsilon} \left(\vec{J}_{source} + \sigma \vec{E} \right) \end{aligned} \tag{10}$$

If we write the vector components of the curl operators in Cartesian coordinates we will obtain the following system of six coupled scalar equations:

$$\begin{aligned}\frac{\partial \vec{H}_{x,y,z}}{\partial t} &= -\frac{1}{\mu}\left[\frac{\partial E_{y,z,x}}{\partial z,x,y} - \frac{\partial E_{z,x,y}}{\partial y,z,x} - \vec{M}_{source_{x,y,z}}\right] \\ \frac{\partial \vec{E}_{x,y,z}}{\partial t} &= \frac{1}{\varepsilon}\left[\frac{\partial H_{z,x,y}}{\partial y,z,x} - \frac{\partial H_{y,z,x}}{\partial z,x,y} - \vec{J}_{source_{x,y,z}}\right]\end{aligned} \tag{11}$$

if we consider that σ^* and σ are equal to zero [1-3, 20].

The system of six coupled partial differential equations forms the basis of the FDTD numerical algorithm for electromagnetic wave interactions with general three-dimensional objects[1-3,19-20].

If we consider the bi-dimensional case when the photonic device is in the X-Z plane and the propagation is made along the Z axis and the Y axis is considered infinite, then the Maxwell equations derive into two sets of independent equation, namely transversal electric (TE) and transversal magnetic (TM) [22-23].

In our paper we studied the only the TE waves. In this case the components of the field are H_x, E_y, $H_z \neq 0$ and the propagation is made along the z axis:

$$\begin{aligned}\frac{\partial E_y}{\partial t} &= \frac{1}{\varepsilon}\left[\frac{\partial H_x}{\partial z} - \frac{\partial H_z}{\partial x}\right] \\ \frac{\partial H_x}{\partial t} &= \frac{1}{\mu_0}\frac{\partial E_y}{\partial z} \\ \frac{\partial H_x}{\partial t} &= -\frac{1}{\mu_0}\frac{\partial E_y}{\partial x}\end{aligned} \tag{12}$$

The Ey field is considered to be the center of the FDTD space cell (Figure 3). The dashed lines form the FDTD cells. The magnetic fields *Hx* and *Hz* are associated with cell edges. The locations of the electric fields are associated with integer values of the indices *i* and *k*. The *Hx* field is associated with integer *i* and (*k* + 0.5) indices. The *Hz* field is associated with (*i* + 0.5) and integer *k* indices [10,11,22].

The numerical analog in equation (12) can be derived from the following relation:

$$\frac{\partial E_y}{\partial t} = \frac{1}{\varepsilon}\left[\frac{\partial H_x}{\partial z} - \frac{\partial H_z}{\partial x}\right] \tag{13}$$

After numerical discretization we obtain:

$$\frac{E_y^n(i,k)-E_y^{n-1}(i,k)}{\Delta t}=\frac{1}{\varepsilon}\frac{H_x^{n-\frac{1}{2}}(i,k+\frac{1}{2})-H_x^{n-\frac{1}{2}}(i,k-\frac{1}{2})}{\Delta z}- \\ -\frac{1}{\varepsilon}\frac{H_z^{n-\frac{1}{2}}(i+\frac{1}{2},k)-H_x^{n-\frac{1}{2}}(i+\frac{1}{2},k)}{\Delta x} \tag{14}$$

where n labels the time steps while the indices i and k label the space steps and along the x and z directions, respectively. The time step is determined by the Courant limit Δt [13-14].

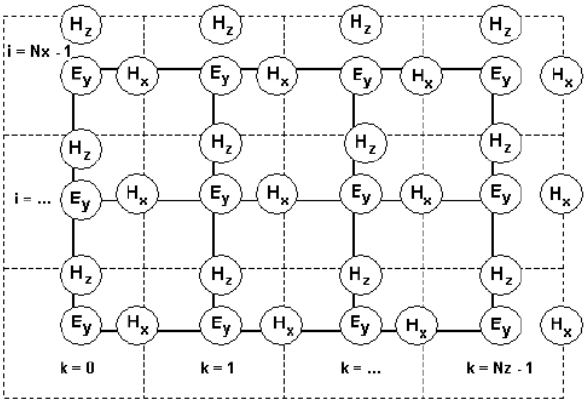

Fig. 3. The location of the TE fields in the computational domain [22-23]

The components of the field can be written as:

$$E_y^n(i,k)=E_y^{n-1}(i,k)+\frac{\Delta t}{\varepsilon\Delta z}\left[H_x^{n-\frac{1}{2}}(i,k+\frac{1}{2})-H_x^{n-\frac{1}{2}}(i,k-\frac{1}{2})\right]- \\ \frac{\Delta t}{\varepsilon\Delta x}\left[H_z^{n-\frac{1}{2}}(i+\frac{1}{2},k)-H_z^{n-\frac{1}{2}}(i-\frac{1}{2},k)\right] \\ H_x^{n+\frac{1}{2}}(i,k+\frac{1}{2})=H_x^{n-\frac{1}{2}}(i,k+\frac{1}{2})+\frac{\Delta t}{\mu_0\Delta z}\left[E_y^n(i,k+1)-E_y^n(i,k)\right] \\ H_z^{n+\frac{1}{2}}(i+\frac{1}{2},k)=H_x^{n-\frac{1}{2}}(i+\frac{1}{2},k)+\frac{\Delta t}{\mu_0\Delta x}\left[E_y^n(i+1,k)-E_y^n(i,k)\right] \tag{15}$$

The quality factor of an optical ring-resonator can be described quantitatively as:

$$Q=\frac{n_{eff}}{\lambda}L\cdot F, \tag{7}$$

where n_{eff} is the effective refractive index of the material, L is the circumference of the ring, λ is the wavelength and F the finesse. The method to determine the finesse is well described in [10-11].

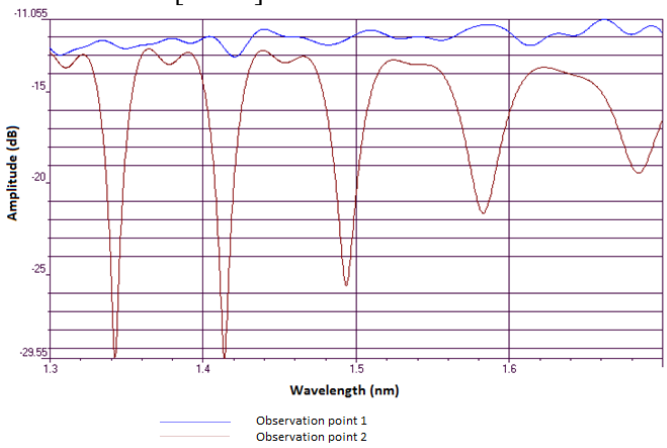

Fig. 4. The evolution of amplitude versus wavelength for 2 observation points (the Observation Point 1 is located at the input and Observation Point 2 at the output).

In Fig. 4 we presented an example of the evolution of amplitude versus wavelength at the input and at the output of the waveguide (at the input the signal is almost flat, while at the output we obtained the wavelength resonances). The quality factor is obtained, numerically, as the ratio between the free spectral range (FSR defined as the distance between two resonances from Fig. 4 on Observation Point 2) and the full width half maximum (FWHM).

3. Silicon on insulator micro-ring resonator

For our numerical simulation we considered a micro-ring resonator as seen in Fig.5. The length of the waveguide was considered to be 15 μm and the radius of the ring to be 2,02 μm. Consequently, we obtain the value for the length of the ring to be equal to $L = 2\pi r = 12{,}7\ \mu m$.

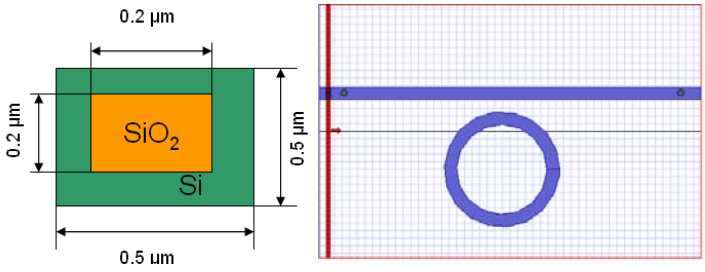

Fig. 5. Geometrical section - silicon on insulator micro-ring resonator. the width of the ring is equal to 0,5 μm ; b. the gap between the ring and the waveguide is equal to 0,51 μm

We considered the input signal a Gaussian Modulated Continuous Wave. The time step size was equal to $1{,}55 \cdot 10^{-16}$ with 5000 time steps.

The refractive index of the *Si* was considered 3,47 and of SiO_2 1,45. The obtained value for the effective refractive index of the structure is equal to 3,03.

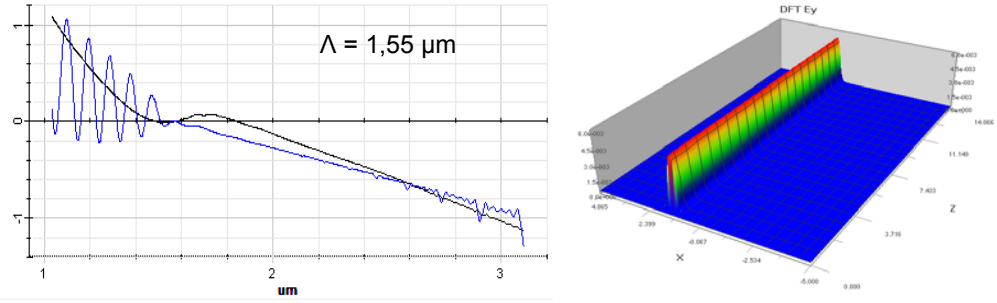

a. b.

Fig. 6. a. Evolution of the amplitude versus the wavelength for telecom based applications; b. Evolution of the E_y component versus the propagation distance for 1,55 μm.

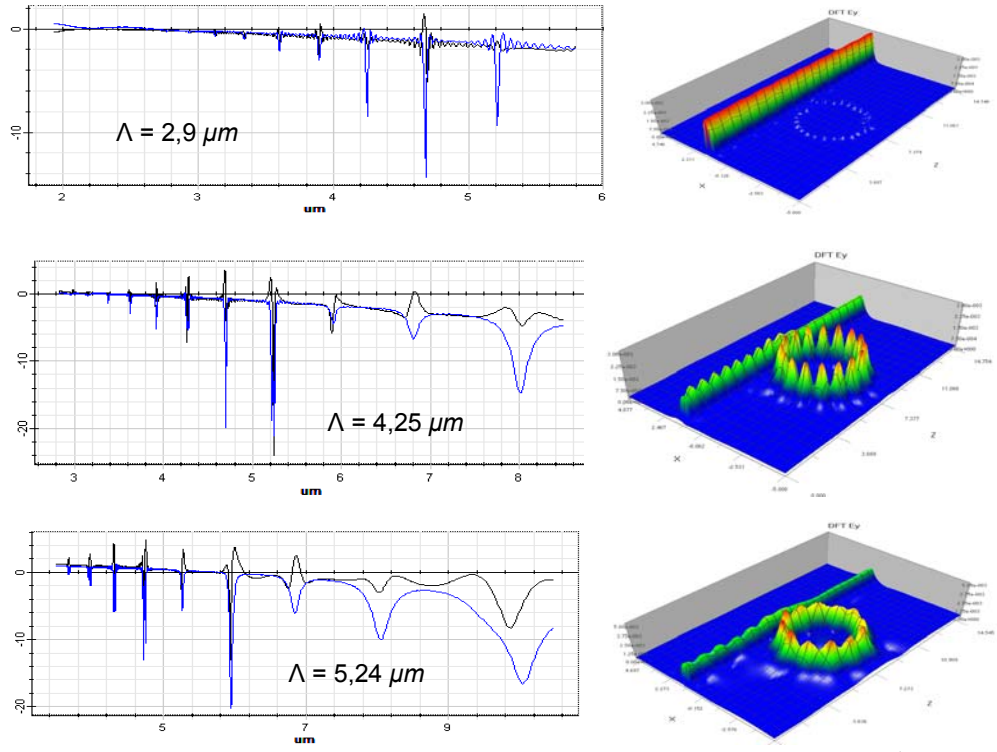

a. b.

Fig. 7. a. Evolution of the amplitude versus the wavelength for different wavelengths; b. Evolution of the E_y component versus the propagation distance for different wavelengths.

The case of telecommunication wavelength is presented in Fig. 6. We can observe that the waveguide has a normal behaviour and transmits the entire signal from the input to the output of the waveguide smoothly.

If we increase the wavelength to 2.9 μm we observe a tiny signal in the ring, but if we choose to simulate at the resonance wavelengths (4,25 μm and 5,24 μm) we find out that the signal in the ring is higher than the signal in the waveguide. In the cases presented in Fig. 7 we obtained quality factors between 200 and 500.

4. Silicon on insulator micro-ring resonator in the presence of a second order and third order waveguide materials

For a waveguide with a nonlinear material (polymer PBZT) of second order (with relative linear permittivity = 2,7225 and second order susceptibility = $5*10^{-13}$ (m/V)) we observed, even at telecommunication wavelength, a dispersion of the signal (Fig. 8).

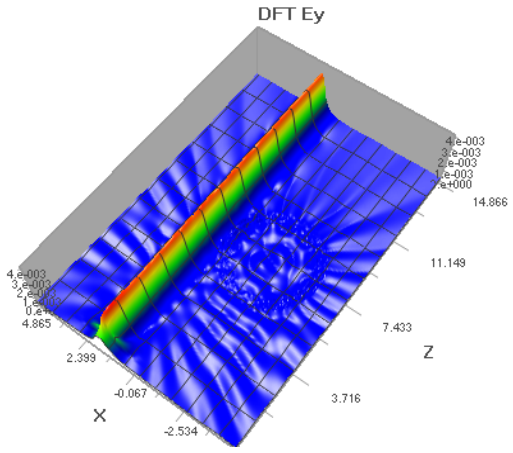

Fig. 8. Evolution of the E_y component versus the propagation distance at 1,55 μm for the second order nonlinear material in the waveguide.

If we considered the resonance wavelength of 2,5 μm, we obtained a higher quality factor for the micro-ring. From Fig. 10 we obtained a quality factor of around 550. For bio-sensing applications the quality factor must have orders of magnitude of thousands. These micro-rings can be used to detect cancer molecules, due to the following propriety: the transmission spectrum of the micro-ring is very sensitive to the refractive index changes.

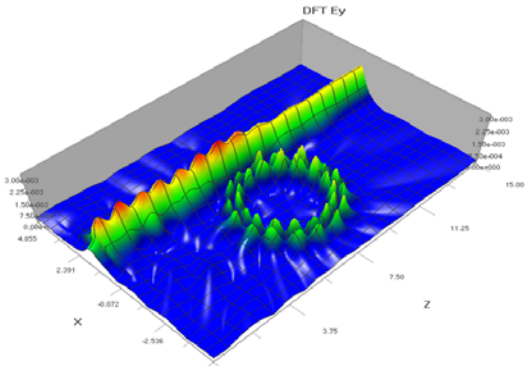

Fig.9. Evolution of the E_y component versus the propagation distance at 2,5 μm for the second order nonlinear material in the waveguide.

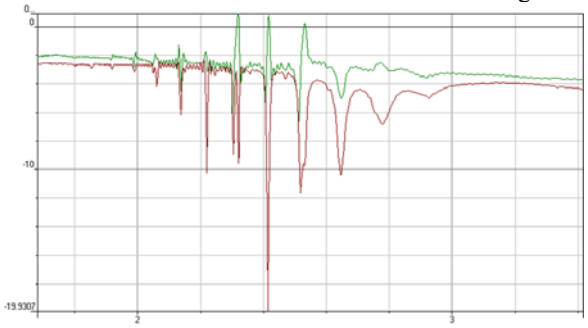

Fig.10. Relative power versus distance at 2,5 μm for the second order nonlinear material in the waveguide

The same waveguide was analyzed considering the third order nonlinearity (with relative linear permittivity = 2,7225 and third order susceptibility = $1{,}25*10^{-18}$ (m^2/V^2)). As in the previous case we observed, even at telecommunication wavelength, a dispersion of the signal.

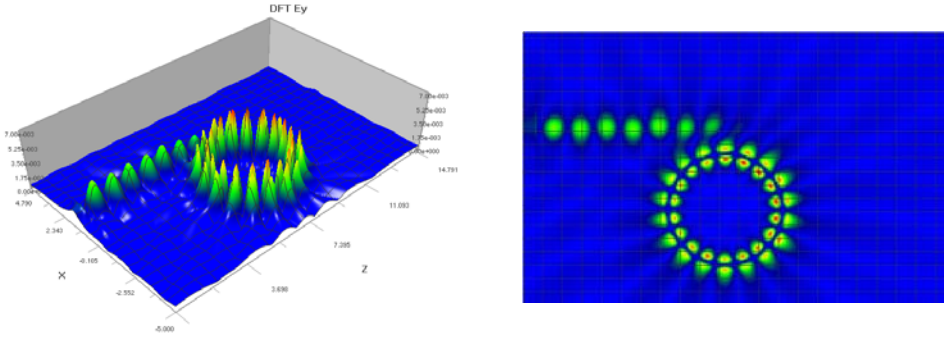

a. b.

Fig. 11. a. Evolution of the E_y component versus the propagation distance at 2,41 μm; b. The projection (X, Z axes) at 2,41 μm.

Considering the resonance wavelength of 2,41 μm we obtained a high quality factor of around 720 (Fig. 11). At this resonance wavelength we can observe that the signal remains in the micro-ring, but if we choose another resonance wavelength of 2,5 μm (Fig. 12) we observe that the quality factor decreases. Consequently, in this case we obtained a better signal in the waveguide.

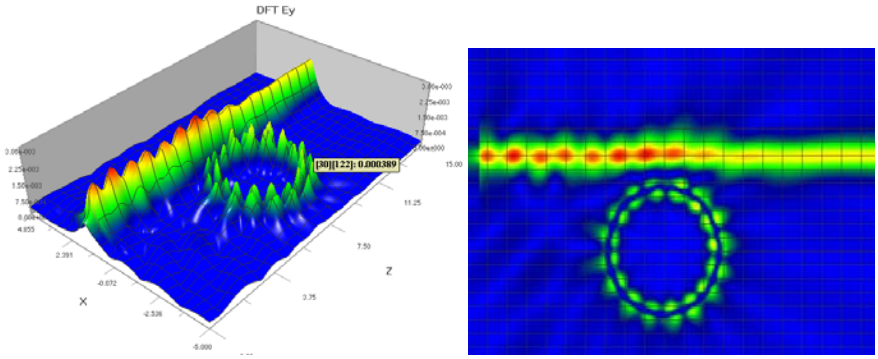

a. b.

Fig. 12. a. Evolution of the E_y component versus the propagation distance at 2,5 μm;
b. The projection (X, Z axes) at 2,5 μm .

5. Conclusions

In this paper we studied the nonlinear behaviour in Silicon-on-Insulator based micro-ring resonators. For our simulations we used he Finite Difference Time-Domain Method, a powerful mathematical tool to solve Maxwell equations.

Nonlinear effects are of great interest, due to their importance in different types of applications, ranging from filters to sensing. For different wavelengths our simulations revealed good quality factors.

The cost to manufacture these photonic devices is still high and here we highlighted the importance of numerical modelling. Finite Difference Time-Domain Method can be used by designers to obtain optimal parameters for their applications.

REFERENCES

[1] *Dennis M. Sullivan*, Electromagnetic simulations using FDTD Method, Wiley-IEE Press, New York, 2000.

[2]. *P.E. Sterian*, "Photonics", vol.**1**, (in Romanian), Printech Publishing House, Bucharest, 580 p., (ISBN 973-652-161-3), 2000.

[3] *Allen Taflove, Susan C. Hagness*, Computational Electrodynamics: The Finite-Diffrence Time-Domain Method Second Edition, Artech House INC., London, 2000.

[4] *S. C. Hagness, D. Rafizadeh, S. T. Ho and A. Taflove*, FDTD Microcavity Simulations: Design and Experimental Realization of Waveguide-Coupled Single-Mode Ring and Whispering-Gallery-Mode Disk Resonators, Journal of Lightwave Technology, vol. **15**, no. 11, pp. 2154 - 2165, 2007.

[5] *A.R. Sterian* "Coherent Radiation Generation and Amplification in Erbium Doped Systems", Advances in Optical Amplifiers, Paul Urquhart (Ed.), ISBN: 978-953-307-186-2, InTech,VIENNA, 2011.

[6] *Andrea Melloni, Francesco Morichetti, Mario Martinelli*, Linear and nonlinear pulse propagation in coupled resonator slow-wave optical structures, in Optical and Quantum Electronics, vol. **35**, pp. 365-379, 2003.

[7] *Christian Koos, Masafumi Fujii, Christopher G.Poulton, Ralf Steingrueber, Juerg Leuthold, Wolgang Freude*, FDTD-Modelling of Dispersive Nonlinear Ring Resonators: Accuracy Studies and Experiments, IEE Journal of Quantum Electronics, vol **42**, no. 12, pp. 1215 - 1223, 2006.

[8] *A. Sterian, P. Sterian,* "Mathematical Models of Dissipative Systems in Quantum Engineering**",** Mathematical Problems in Engineering, **vol**. 2012, Article ID 347674, 12 pages, doi:10.1155/2012/347674, 2012.

[9] *Shiyun Lin, Ethan Schonbrun, Kenneth Crozier*, Optical Manipulation with Planar Silicon Micro-ring Resonators, Nano Letters, pp. 2408–2411, 2010.

[10] *Yuntao Li, Yingtao Hu, Xi Xiao, Zhiyong Li, Yude Yu, Jinzhong Yu,* Cascaded Passive silicon microrings for large bandwidth slow light devices, Journal of Physics: Conference Series vol. **276**, no. 1, pp. 12068-12071, 2011.

[11] *G. Priem, P. Dumon, W. Bogaerts, D. Van Thourhout, G. Morthier, R. Baets,* Optical bistability and pulsating behaviour in Silicon-On-Insulator ring resonator structures, Optics Express, vol. **13**, no. 23, pp. 9623-9628, 2005.

[12] *Thomas Van Vaerenbergh, Martin Fiers, Pauline Mechet, Thijs Spuesens, Rajesh Kumar, Geert Morthier, Benjamin Schrauwen, Joni Dambre, Peter Bienstman*, Cascade excitability in microrings, Optics Express, **vol. 20**. no. 18, pp. 20292-20308, 2012.

[13] *Dominik G. Rabus*, Integrated Ring Resonators. The Compendium, Springer-Verlag Berlin Heidelberg, 2007.

[14] *B. Lazar, P. Sterian*,"The multimode photonic crystal resonator and its application to unidirectional optical energy transfer", J. Optoel. Adv. Mat., Vol. **13,** Issue**:** 1-2, Pages: 32-40, 2011.

[15] *R. F. Stancu, P. Sterian,* "Beam propagation and non-linear effects in photonic crystal optoelectronic devices", J. Optoel. Adv. Mat., Vol. **14,** Issue: 3-4, Pages: 371-375, 2012.

[16] *B. Lazar, P. Sterian,* "Photonic crystal band-stop filter with monomode resonator", J. Optoel. Adv. Mat., Vol.**12,** Issue: **1** Pages: 24-30, 2010.

[17] *B. Lazar, P. Sterian,* "Photonic crystals resonant cavities. Quality factors",Vol. **10**,Issue**:** 1, J. Optoel. Adv. Mat., Pages: 44-54, 2008.

[18] *R. F. Stancu, P. Sterian,* "Photonic crystal optoelectronic devices and circuits for student training", Optoel. Adv. Mat., -Rapid Comm.Vol.**4,** Issue: 12, Pages: 2114-2117, 2010.

[19] *B. Lazar, P. Sterian,* "Band gaps in 2D photonic crystals with square symmetry", J. Optoel. Adv. Mat., Vol. **12,** Issue: 4, Pages: 810-817, 2010.

[20] *Andreea Fazacas, Paul Sterian*, Finite-Difference Time-Domain Method (FDTD) used to Simulate Micro-ring Resonator for Student Applications, J. Optoel. Adv. Mat., vol. **14**, no. 3-4, pp. 344 – 349, 2012.

[21] *Andreea Fazacas, Paul Sterian*, Second and third order dispersion effects analyzed by the split-step Fourier methor for soliton propagation in optical fibers, J. Optoel. Adv. Mat., vol. **14**, no. 3-4, pp. 376 – 382, 2012.
[22] http://www.optiwave.com/products/fdtd_overview.html
[23] OptiFDTD Technical Background and Tutorials